



THE DYNAMIC RESPONSE OF A CONTINUOUS PLATE FOR DIFFERENT SURFACE STATES

Moussa GUEBAILIA^{1,2}, Nouredine OUELAA²

¹ Kasdi Merbah University Ouargla, guebailiamoussa2@hotmail.com

² Mechanics & Structure Laboratory Guelma University, n_ouelaa@yahoo.fr

Abstract

Several dynamic effects can be generated and simply observed by the passage of an external mobile exciter forces with different speeds on the surface of an orthotropic continuous plate. In the present paper one illustrates the dynamic behaviour of a thin, orthotropic, multi-span plate, subjected to the passage of moving exciters. In this model, the roughness of the surface of the plate is considered as the contact surface between mobile exciter and the plate. The modal and Newmark integration methods are used in order to solve the coupled plate–exciter equations of motion. One presents especially results which show clearly the influence of the surface states on the dynamic behaviour of the plate and also the generated interaction forces due to the surface roughness. In this paper one presents also the influence of the mobile exciter speeds on the plate dynamic response.

Keywords: dynamic behaviour; interaction force; plate; surface irregularities; dynamic response

1. INTRODUCTION

Many important parameters can be extracted and evaluated from the dynamic analysis of bridges. Moreover, the interaction bridge – mobile exciter can be amplified by other factors.

In the references [1, 2], the mobile exciter was modelled by a three-dimensional dynamic model with two axles and seven degrees-of-freedom dofs compliant with the standard H20-44 (2005) [3]. The natural frequencies and modes shapes were calculated by the Rayleigh-Ritz method, and the dynamic response was obtained by the modal superposition method [1, 2].

Zhu et al. (2001) [1] and Marschillo et al. (1999) [2] used the variational method of Rayleigh-Ritz to determine the natural frequencies and mode shapes of the bridges using the Eigen modes of the beams as approximation functions. These authors decomposed into a product the two admissible functions, which are the Eigen modes of a continuous beam simply supported and a free beam mode.

Chompooming et al. (1995) [4] present an analysis of the bridge-vehicle interaction problem taking into account the dynamic effects due to vehicle rebound caused by road irregularity and the variation of the vehicle speed. The spatial discretization of the differential equations governing the bridge-vehicle system is based on the finite element method. The solution is based on the Newmark method (temporal integration technique) is referred to as the numerical method of the lines. As the bridge-vehicle interaction introduces non-linearity in the formulation, the authors adopt a

multi-factor prediction-correlation scheme in the resolution procedure to obtain accurate results.

Burdzik (2014) [5] studies in this work the case of multiple sources of vibration interacting on vehicle and vibration transfer into driver and passengers. During the research the passenger car was driven on special test track. It were recorded the vibration signals in 3 orthogonal axes. It allows evaluating exposure on vibration in frequency bands close to natural frequency of chosen human organs. The analysis of time-frequency distribution of the vibration allows separating the main components of the signal. The paper presents the results of comparison of RMS value of vibration for different axes in measurement points on floor panel.

The dynamic behaviour of bridges subjected to road traffic was studied by Broquet (1999) [6], in which a two-stage evaluation of the bridge slab was proposed. In Stage 1, for situations similar to those analysed in that study, a simplified evaluation was applied. This employed a static analysis using an increased load based on a dynamic amplification factor. If the simplified evaluation could not be applied, a second stage (Stage 2) was adopted to evaluate the deck slab using a dynamic analysis, which took the form of either a numerical or an experimental approach [6]. That work evaluated the influence of roadway flatness and the load and speed of trucks on the dynamic response of the deck slab [6].

Konieczny and al. (2015) [7], present results of a vibroacoustic signal analysis of the unsprung mass in a car actuated by harmonic kinematic vibrations. They used different tire pressures during the experiments. The authors applied the short time Fourier transform method with superposition of the

Hanning windows combined with the zero complement method. With reference to the STFT spectrum, values of the unsprung mass resonance frequency were identified. The results of the experiments described in the publication are particularly useful for the personnel of vehicle service stations, especially that they relate to the effect of tire pressure changes occurring in a vehicle with a hydropneumatic suspension system on the vibration test results.

In a vibro-acoustic study on a railway bridge excited by the passage of train, Ouelaa et al. (2006) [7] modelled the deck rail system including the train weight, the viscoelastic mobile exciter suspension, and the track irregularities. To resolving the equations of coupled motion, the modal superposition and Newmark methods were used. They show that the track irregularities disturb significantly the transverse movement of the mobile exciters, whereas they have a very small influence on the dynamic behaviour of the bridge [8].

1. PLATE MODEL

The assumptions proposed by Zhu et al. (2001) and Marschillo et al. (1999) [1, 2] to model the plate vibrations are the modelling basis of this work.

The model used is an orthotropic, thin plate with three spans (Figure 1). The equation of the plate motion is written in Eqn 1:

$$\bar{m} \frac{\partial^2 w}{\partial t^2} + c \frac{\partial w}{\partial t} + D_x \frac{\partial^4 w}{\partial x^4} + 2H \frac{\partial^4 w}{\partial x^2 \partial y^2} + D_y \frac{\partial^4 w}{\partial y^4} = - \sum_{k=1}^{nf} F_{pk}^{int} \delta(x-x_k(t), y-y_k) \quad (1)$$

Where

$\bar{m} = \rho h$ is the mass density of the plate;

$D_x = E_x h^3 / 12 (1 - \nu_{xy} \nu_{yx})$,

$D_y = E_y h^3 / 12 (1 - \nu_{xy} \nu_{yx})$ are flexural rigidities according to the x and y directions;

$H = \nu_{xy} D_y + 2D_{xy}$ is the equivalent rigidity;

c is the damping ratio of the plate;

F_{pk}^{int} is the interaction force between the kth exciter wheel and the plate,

$(x_k(t), y_k)$ is the position of the kth interaction force;

ν_{xy} and ν_{yx} are the Poisson's coefficients according to the x- and y- directions, respectively;

$D_{xy} = G_{xy} h^3 / 12$ is the flexural rigidity for the x-y plane;

G_{xy} is the shear modulus in bending in the x-y plane;

E_x and E_y are the Young's moduli in the x- and y- directions.

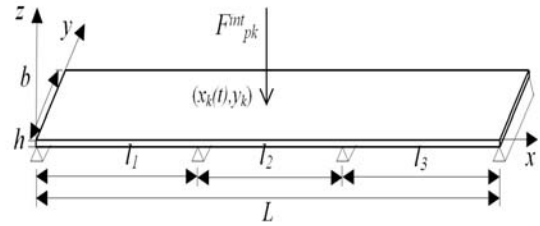


Fig. 1. Plate model.

Mobile exciters are assumed to move along the plate in linear direction meaning that y_k is constant. The mobile exciter speed is considered constant. Thus, $x_k(t) = v_x \cdot t_k$ (where v_x is the linear speed of the mobile exciter, and t_k is the time at the point k).

The equation of motion (1) is solved using modal superposition and Newmark's method. The vertical displacement of the plate presented in Eqn (2).

$$w(x, y, t) = \sum_{i=1}^n \sum_{j=1}^m \phi_{ij}(x, y) \cdot q_{ij}(t) \quad (2)$$

Where $\phi_{ij}(x, y)$ are the modes shapes of a thin, multi-span orthotropic plate, which are associated with the natural angular frequencies ω_{ij} .

$q_{ij}(t)$ are the generalized coordinates.

Substituting expression (2) into the equation of motion (1) and multiplying both sides by $\phi_{kl}(x, y)$, Eqn (3) is generated when the equation is integrated over the entire surface of the plate.

$$\begin{aligned} & \iint_S \bar{m} \sum_{i,j=1}^{n,m} \phi_{ij}(x, y) \ddot{q}_{ij}(t) \phi_{kl}(x, y) dx dy + \\ & \iint_S c \sum_{i,j=1}^{n,m} \phi_{ij}(x, y) \dot{q}_{ij}(t) \phi_{kl}(x, y) dx dy + \\ & \iint_S D_x \sum_{i,j=1}^{n,m} \frac{\partial^4 \phi_{ij}}{\partial x^4} q_{ij}(t) \phi_{kl}(x, y) dx dy \\ & + 2 \iint_S H \frac{\partial^2 \phi_{ij}}{\partial x^2} \frac{\partial^2 \phi_{ij}}{\partial y^2} q_{ij}(t) \phi_{kl}(x, y) dx dy + \\ & \iint_S D_y \sum_{i,j=1}^{n,m} \frac{\partial^4 \phi_{ij}}{\partial y^4} q_{ij}(t) \phi_{kl}(x, y) dx dy \\ & = - \iint_S \sum_{k=1}^{nf} F_{pk}^{int} \phi_{kl} \delta(x-x_k(t), y-y_k) \end{aligned} \quad (3)$$

The orthogonality of natural modes guarantees the decoupling of modal responses and gives the relations in Eqn (4):

$$\iint_S \bar{m} \phi_{ij}(x, y) \phi_{kl}(x, y) dx dy = \begin{cases} 0 & \text{for } ij \neq kl \\ M_{ij} & \text{for } ij = kl \end{cases}$$

$$\iint_S c\phi_{ij}(x,y)\phi_{kl}(x,y)dxdy = \begin{cases} 0 & \text{for } ij \neq kl \\ C_{ij} = 2\xi_{ij}\omega_{ij}M_{ij} & \text{for } ij = kl \end{cases}$$

$$\iint_S \left(D_x \frac{\partial^4 \phi_{ij}}{\partial x^4} + 2H \frac{\partial^4 \phi_{ij}}{\partial x^2 \partial y^2} + D_y \frac{\partial^4 \phi_{ij}}{\partial y^4} \right) \phi_{kl}(x,y) dxdy = \begin{cases} 0 & \text{for } ij \neq kl \\ \omega_{ij}M_{ij} = K_{ij} & \text{for } ij = kl \end{cases}$$

(4)

Where $\xi_{ij} = c / 2\bar{m}\omega_{ij}$, the modal damping coefficients of the bridge.

By applying orthogonality conditions (4), the terms that satisfy $ij \neq kl$ disappear, and the modal equations (i, j) are decoupled from equation (3), as shown in Eqn (5):

$$M_{ij}\ddot{q}_{ij}(t) + C_{ij}\dot{q}_{ij}(t) + K_{ij}q_{ij}(t) = F_{ij}(t) \quad (5)$$

Where

$$M_{ij} = \iint_S \bar{m}\phi_{ij}^2(x,y)dxdy$$

$$C_{ij} = \iint_S c\phi_{ij}^2(x,y)dxdy = 2\xi_{ij}\omega_{ij}M_{ij}$$

$$K_{ij} = \iint_S \left(D_x \frac{\partial^4 \phi_{ij}}{\partial x^4} + 2H \frac{\partial^4 \phi_{ij}}{\partial x^2 \partial y^2} + D_y \frac{\partial^4 \phi_{ij}}{\partial y^4} \right) \phi_{ij} dxdy = M_{ij}\omega_{ij}^2$$

$$F_{ij} = -\iint_S \sum_{k=1}^{nf} F_{pk}^{int} \delta(x-x_k(t), y-y_k) \phi_{ij}(x,y) ds$$

$$= -\sum_{k=1}^{nf} F_{pk}^{int}(x_k, y_k) \phi_{ij}(x_k, y_k) \quad (6)$$

Where M_{ij} , C_{ij} , K_{ij} and F_{ij} are the modal masses, damping, stiffness and forces respectively.

The determination of the natural frequencies and mode shapes are identified by the estimate method presented in Guebailia et al. (2013) [10]

3. SOLVING METHOD ALGORITHM

To solve the coupled equations of motion one suggests following these steps:

- Input data of plate, mobile exciter,...
- Calculate: $D_x, D_y, H, D_{xy}, G_{xy}, \bar{m}$
- Choose the number of Eigenmodes: n, m
- Determine the natural frequencies ω_{ij} ,
- Calculate the mode shapes ϕ_{ij}
- Select the passage speed,
- choose the time step Δt , parameters (γ, β) and the precision ε ,
- Calculate the matrixes of mass, stiffness and modal damping of the plate and mobile exciter,
- Specify the initial conditions.

Plate: $\{q\}_0, \{\dot{q}\}_0, \{\ddot{q}\}_0$, Displacements, velocities and accelerations generalized (modal coordinates).

Mobile exciter: $\{Z_v\}_0, \{\dot{Z}_v\}_0, \{\ddot{Z}_v\}_0$, Mobile exciter' DOFs

- Choose the mobile exciter trajectory on the plate,

- For each time step $t = t + \Delta t$:

Determine the x position of the mobile exciter on the plate,

Calculate the profile of the plate surface at each point of contact,

-For each iterate k:

Solve this by Newmark's method,

$$[M_v]\{\ddot{Z}_v\} + [C_v]\{\dot{Z}_v\} + [K_v]\{Z_v\} = \{F_v^{int}\}$$

Calculate the interaction forces on the plate to mobile exciter by the following expression:

$$\{F_p^{int}\} = \{F_g\} + \{F_p\}$$

where

$\{F_g\}$ = force vector due to the effects of gravity,

$\{F_p\}$ = force vector exerted by the plate

Solve by Newmark's method

$$\ddot{q}_{ij} + 2\xi_{ij}\omega_{ij}\dot{q}_{ij} + \omega_{ij}^2 q_{ij} = \frac{1}{M_{ij}} F_{ij}$$

With,

$$F_{ij} = -\sum_{k=1}^4 F_{pk}^{int}(x_k, y_k) \phi_{ij}(x_k, y_k)$$

- Calculate the plate's vertical displacement:

$$w(x, y, t) = \sum_{i=1}^n \sum_{j=1}^m \phi_{ij}(x_k, y_k) q_{ij}(t)$$

and verify the convergence:

$$\left| w^{(\bar{k}+1)}(x, y, t) - w^{(\bar{k})}(x, y, t) \right| \leq \varepsilon$$

4. RESULTS

To validate the presented model, the plate and mobile exciter are taken from Zhu et al. [1].

Surface data:

Length L = 78m,

Width b = 13.715m,

Span's lengths $l_1 = l_3 = 24m$ and $l_2 = 30m$,

Thickness h = 0.21157m,

Mass per unit of length

$$\bar{m} = 3265.295 \text{kg/m}^3,$$

The flexural rigidity according to x

$$D_x = 2.415 \cdot 10^9 \text{Nm},$$

The flexural rigidity according to y

$$D_y = 2.1807 \cdot 10^7 \text{Nm},$$

The flexural rigidity for the x-y plane

$D_{xy} = 1.1424 \cdot 10^8 \text{Nm}$,
 The Poisson's ratio $\nu_{xy} = 0.3$,
 Young moduli
 $E_x = 3.0576 \cdot 10^{12} \text{N/m}^2$, $E_y = 2.7607 \cdot 10^{10} \text{N/m}^2$,
 The shear modulus in bending for the x - y
 plane $G_{xy} = 1.4475 \cdot 10^{11} \text{N/m}^2$.

Mobile exciter data:

$m_1 = 600 \text{kg}$, $m_2 = 1000 \text{kg}$ the masses of the wheel
 with axles front and rear, respectively,
 $m_v = 17000 \text{kg}$, $I_{\theta v} = 9 \cdot 10^4 \text{kg}$, $I_{av} = 1.3 \cdot 10^4 \text{kg}$ the
 mass and the moments of inertia of the mobile
 exciter block,
 $I_{\theta 1} = 550 \text{kg.m}^2$, $I_{\theta 2} = 600 \text{kg.m}^2$ the moments of
 inertia of the axles of the front and rear
 respectively,
 $K_{p1} = K_{p2} = 7.85 \cdot 10^5 \text{N/m}$, $K_{p3} = K_{p4} = 5.7 \cdot 10^5 \text{N/m}$ tires'
 rigidities,
 $K_{s1} = K_{s2} = 1.16 \cdot 10^5 \text{N/m}$, $K_{s3} = K_{s4} = 3.73 \cdot 10^5 \text{N/m}$
 suspensions' rigidities,
 $C_{p1} = C_{p2} = 2.5 \cdot 10^4 \text{Ns/m}$, $C_{p3} = C_{p4} = 3.5 \cdot 10^4 \text{Ns/m}$ tires'
 damping,
 $C_{s1} = C_{s2} = 1.0 \cdot 10^2 \text{Ns/m}$, $C_{s3} = C_{s4} = 2.0 \cdot 10^2 \text{Ns/m}$
 suspensions' damping,
 $S_{p1} = S_{p2} = 2.05 \text{m}$ tires spacing of the mobile exciter
 front and rear axles, respectively,
 $S_1 = S_2 = 1.41 \text{m}$ legs spacing of the mobile exciter
 front and rear axles, respectively,
 $S_x = 4.73 \text{m}$ spacing between the mobile exciter front
 and rear axles,
 $a_1 = 0.67 \text{m}$, $a_2 = 0.33 \text{m}$ eccentricities,
 Stability parameters of Newmark's method in all
 calculation steps were as follows:
 $(\gamma = 0.5, \beta = 0.25)$

4.1. Dynamic response of the plate

Figures 2 presents the dynamic displacements
 on the plate, obtained by presented work with a
 30m/s mobile exciter speed at different roadway
 irregularities. The roughness did not have a major
 effect on the dynamic displacement of the plate [8]
 (Fig. 2).

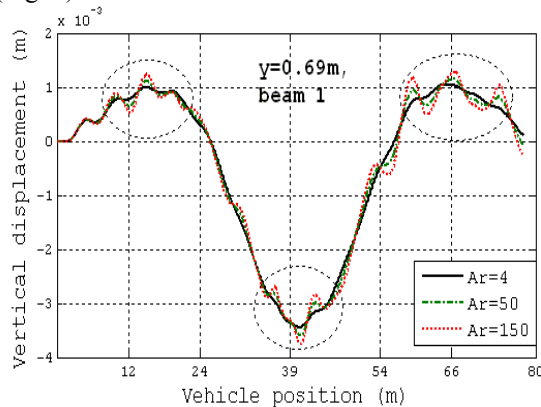


Fig. 2. plate dynamic displacement

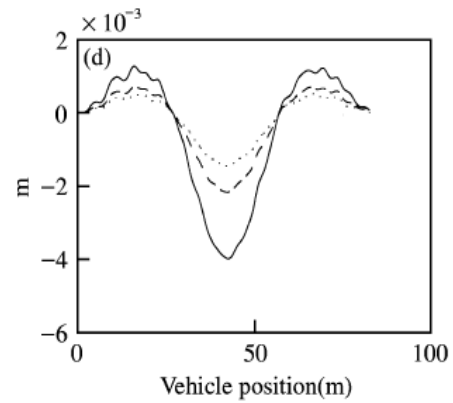


Fig. 3. Dynamic displacement [1].

Figure 4 presents the superposition of the
 dynamic displacement obtained by the CLEF [12]
 and presented method.

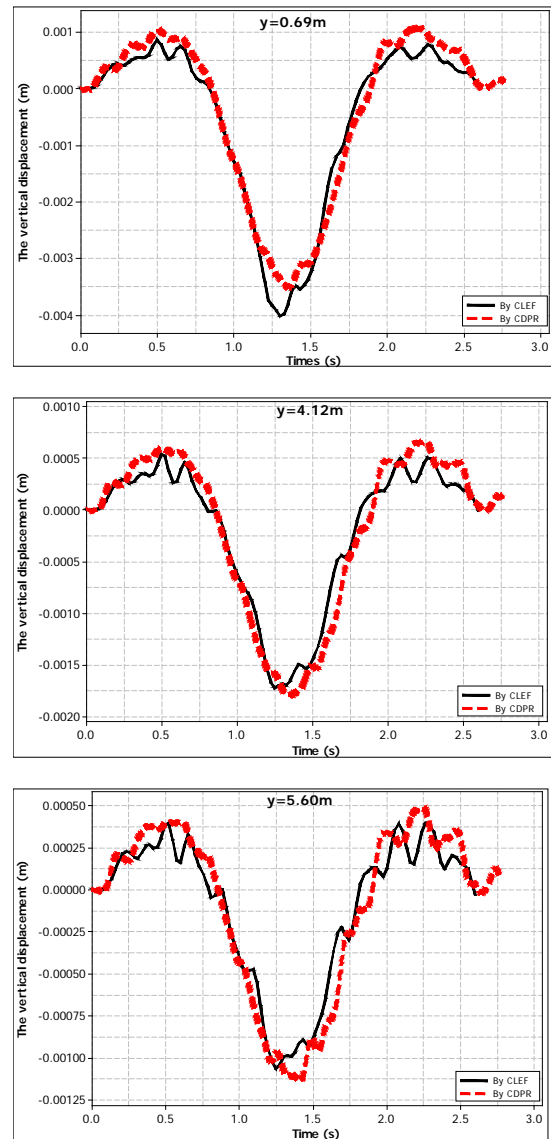


Fig. 4. The superposition of the dynamic displacement obtained by the CLEF and presented method (speed 30m/s, bad roadway conditions)

4.2. Interaction forces

Figure 5, presents an overview of interaction forces that were applied by the right front and rear wheels of the mobile exciter moving on the plate.

The mobile exciter moved at a speed of 30m/s, on a trajectory of $y = 0.69$ m on a roadway with a roughness profile of a medium condition. Where Ar is in the order of 10^{-6} m³/cycle for the two wheels, and the interaction force varied with time with respect to mobile exciter passage, in part dependent upon the position of the wheel around an average value, which corresponds with the static force.

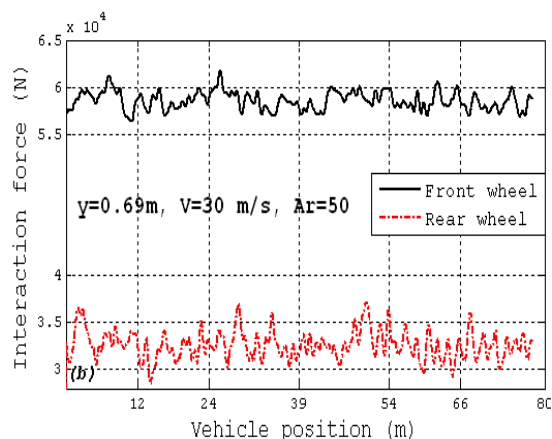


Fig. 5. Interaction forces.

Figure 6 presents the significant influence of the pavement roughness on the interaction forces. For a deteriorated roadway, the interaction force exceeded that of a road of good condition by 1500 - 3000N.

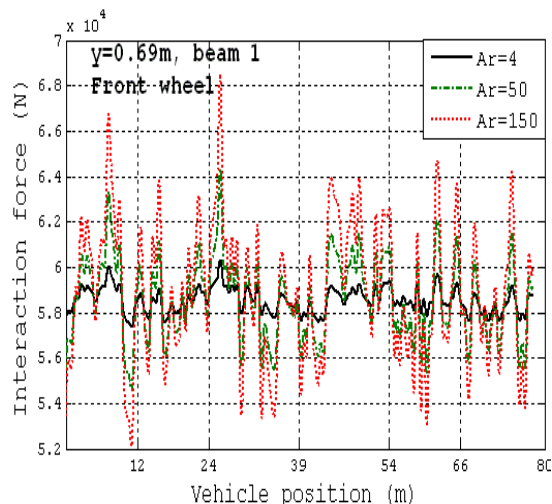


Fig. 6. Interaction forces for different roadway conditions.

The interaction forces obtained with different velocities are presented in Fig. 7.

Notably, for the same road conditions, increasing the speed beyond 30 m/s caused

significant increases in the interaction force for both the front and rear wheels.

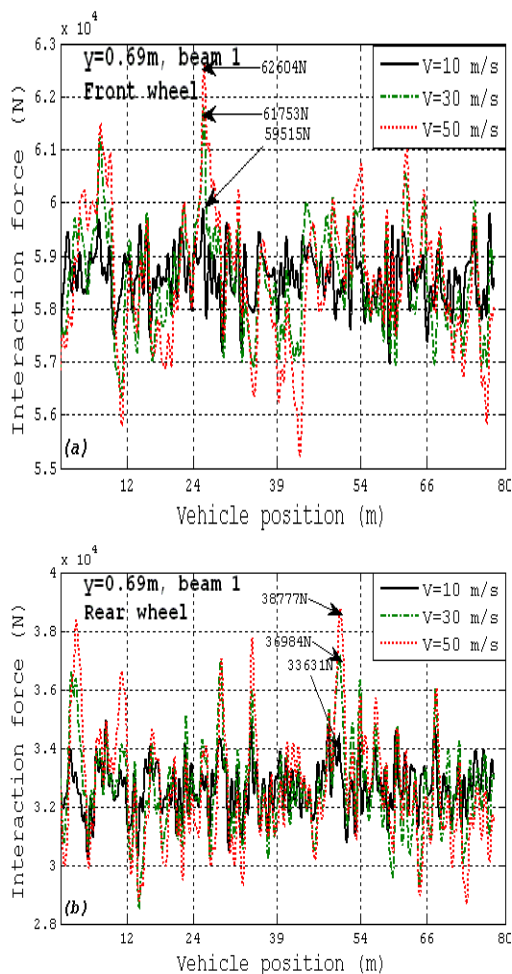


Fig. 7. Interaction forces for different velocities on the middle of the second span.

5. CONCLUSION

By comparing the dynamic response obtained herein with that of Zhu et al.[1], only small differences in the minima and maxima were observed and were likely due to the exclusion of the torsional modes (intermodal coupling) by Zhu et al. [1].

The dynamic displacements of the plate for three trajectories were in good agreement when compared to the software CLEF. The roughness did not have a major effect on the dynamic displacement of the plate but did strongly influence the mobile exciter axle and the plate-mobile exciter interaction forces, especially at speeds in excess of 30 m/s (both front and rear wheels).

The interaction force varied with mobile exciter passage and depended upon the wheel position considering an average value corresponding to the static force F_s for the two wheels.

The mobile exciter trajectory influenced the dynamic displacement.

The method proposed herein uses a local estimate method for the position, thereby drastically reducing the number of differential equations of the free motion of the plate to be solved and enables it to be incorporated into structural analysis software, as there is no required integration.

This is a major advantage over approaches that rely upon a Rayleigh-Ritz method.

6. APPENDIXES

6.1 APPENDIX A: ROADWAY PROFILE

The interface between the bridge and the mobile exciter is the profile of the roadway (Irregularities). These irregularities disturb the vertical displacement of the bridge and the mobile exciter in a major way.

One can model the static profile of the roadway by a random process characterized by a power spectral density (PSD) which is used to describe the quality of the roadway surface:

$$r(x_i) = \sum_{k=1}^N \sqrt{4A_k \left(\frac{2\pi k}{L_c \omega_{k0}} \right) \frac{2\pi}{L_c}} \cos(\omega_{sk} x_i + \theta_k)$$

With

A_k is a coefficient of roughness spectrum that characterizes the state of the roadway ($m^3 / cycle$)

ω_{k0} is the discontinuity angular frequency ($\omega_{k0} = 1/2\pi cycle/m$),

ω_{sk} is the wave number ($\omega_{sk} = 2\pi k / L_c cycle / m$),

L_c is the sampling length generally equal to $2L$,

L is the bridge length,

N is the number of discretization points frequency,

θ_k is a random variable that ranges between 0 and 2π .

7.2 APPENDIX B : MOBILE EXCITER MODEL

The mobile exciter is modelled by a dynamic 7 degrees of freedom model, similar to that used by [1, 2 and 12]. The rigid block of the truck has three degrees of freedom which are:

z_v : corresponds to the bounding,

θ_v : corresponds to the pitching,

α_v : corresponds to the roll.

The bouncing and the axle roll of the front and the rear are presented with four degrees of freedom which are: z_1, z_2 : the vertical displacements of

the axles of the front and rear respectively, θ_1, θ_2 : the rotation of the axles of the front and rear respectively.

To determine the mobile exciter-bridge interaction forces, we determine for each point of contact bridge mobile exciter, displacements of the ends of the springs that model tires.

The equations of motion of the mobile exciter model with seven degrees of freedom are obtained by applying the law of dynamic equilibrium of forces and moments for each degree of freedom.

After rearrangement and grouping, the following system is obtained:

$$[M_v]\{Z_v\} + [C_v]\{Z_v\} + [K_v]\{Z_v\} = \{F_v^{int}\}$$

Where $\{F_v^{int}\}$ is the interactions forces vector applied to the mobile exciter, $[M_v]$, $[C_v]$ and $[K_v]$ are respectively the matrices of mass, damping and stiffness of the mobile exciter model.

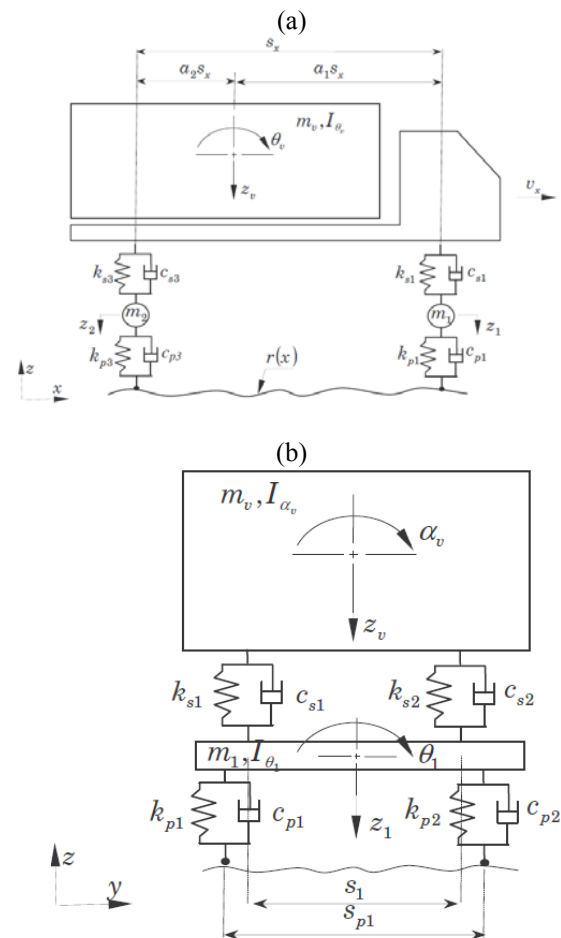


Fig. A.1. Two axle mobile exciter model (AASHTO).
(a) Elevation, (b) Cross sectional [2, 11]

6. REFERENCES

- 1 Zhu XQ, Law SS. Dynamic load on continuous multi-lane bridge deck from moving mobile exciters. *Journal of Sound and Vibration*, 2002; 251(4):697-716.
- 2 Marchesiello S, Fasana A, Garibaldi L, Piombo BAD. Dynamics of multi-span continuous straight Bridges subject to multi-degrees of freedom Moving mobile excitation. *Journal of Sound and Vibration*, 1999, 224(3):541-561.
- 3 American Association of State Highway and Transportation officials. AASHTO LRFD BRIDGE Design specifications. 2005.
- 4 Chompooming K, Yener M. The influence of roadway surface irregularities and mobile exciter deceleration on bridge dynamics using the method of lines. *Journal of Sound and Vibration*, 1995: 183(4): 567-586.
- 5 Burdzik R. Identification of structure and directional distribution of vibration transferred to car-body from road roughness. *Journal of Vibroengineering*, 2014; 16(1):324-333
- 6 Claude Broquet, "Comportement dynamique des dalles de roulement des ponts en béton sollicités par le trafic routier". Thèse de Doctorat 1999, Ecole polytechnique fédérale de Lausanne.
- 7 Ouelaa N, Rezaiguia A, Laulagnet B. Vibro-acoustic modelling of a railway bridge crossed by a train. *Applied Acoustics*, 2006; 67:461-475.
- 8 Konieczny K, Burdzik R, Warczek J, Czech P, Wojnar G, Młyńczak J. Determination of the effect of tire stiffness on wheel accelerations by the forced vibration test method" *Journal of Vibroengineering*, 2015; 17(8).
- 9 Kamel Henchi. Analyses dynamiques des ponts par éléments finis sous les sollicitations des véhicules mobile". Thèse de Doctorat 1995, Université de technologie de Compiègne.
- 10 Guebailia M, Ouelaa N, Guyader JL. Solution of the free vibration equation of a multi span bridge deck by local estimation method. *Engineering Structures EngStruct*, 2913; 48: 695-703.
- 11 Rezaiguia A. Vibroacoustic Modelling of Highway Bridges Crossing by Moving Mobile exciters, Doctorate Thesis, Annaba University, Algeria, 2008.
- 12 CLEF: Software developed by an group of researchers in multi – disciplines at Laval university based of Henchi's works [9] 1995

Received 2017-06-30

Accepted 2017-11-03

Available online 2017-11-06



Dr. GUEBAILIA Moussa

Mechanical doctorate Mechanics & Structure Laboratory of Guelma university.
Kasdi Merbah University of Ouargla.